

## MAGNETIC PROPERTIES OF THE PEROVSKITE OXIDE $\text{PbV}_{1-x}\text{Fe}_x\text{O}_3$ INVESTIGATED BY ELECTRON PARAMAGNETIC RESONANCE SPECTROSCOPY

A. OKOS<sup>1</sup>, OANA RAITA<sup>2</sup>, A. POP<sup>1\*</sup>

**ABSTRACT.** The perovskite oxide  $\text{Pb}(\text{V}_{1-x}\text{Fe}_x)\text{O}_3$  ( $0 \leq x \leq 0.75$ ) was synthesised by solid state reaction under high pressure (HP) – high temperature (HT) conditions. The effect of partial substitution of V with Fe on magnetic properties of  $\text{PbVO}_3$  compound were studied by Electron Paramagnetic Resonance (EPR) spectroscopy measurements.

**Keywords:**  *$\text{PbVO}_3$ , high pressure - high temperature synthesis, EPR spectroscopy*

### INTRODUCTION

The properties of  $\text{ABO}_3$  perovskite oxides can often be improved by introducing magnetic dopants as long as their ferroelectric properties can be maintained.

Bulk  $\text{PbVO}_3$  is known to be a  $\text{PbTiO}_3$ -type structure with a large tetragonal distortion ( $c/a = 1.22$ ), with the V atoms displaced from symmetric O–V–O bonding along the c-axis, [1, 2].

---

<sup>1</sup> Faculty of Physics, Babes-Bolyai University, Str. M Kogălniceanu, Nr. 1, RO-400084 Cluj-Napoca, Romania.

<sup>2</sup> INCDTIM, Str. Donath Nr. 65-103, RO-400293 Cluj-Napoca, Romania.

\* Corresponding author: aurel.pop@phys.ubbcluj.ro

Both theoretical and experimental studies have shown that V ions in bulk  $\text{PbVO}_3$  are arranged in two-dimensional antiferromagnetic (AFM) ordering [3-5]. However, a long magnetic order is difficult to realize in  $\text{PbVO}_3$  samples as it is often coupled to a spin glass phase.[1,6].

The single d electron per  $\text{V}^{IV}$  is localized and ordered into the xy orbital in the basal plane; the in-plane interatomic V–O–V interactions between the localized- electron spins give a broad maximum in the paramagnetic susceptibility near 200 K ,typical of 2D antiferromagnetic interactions [2,7].

If the weak magnetism is caused by the 2D arrangement of the V cations, the substitution could reduce the tendency of the system to form a 2D network and could lead to the onset of a 3D magnetic ordering.

The Fe ion with a large magnetic moment could provide some remnant magnetic moments at the oxygen ions and degrade the magnetic moment of the V ions by Fe–O –V super-exchange interaction [8].

The  $\text{PbV}_{1/2}\text{Fe}_{1/2}\text{O}_3$  sample was previously synthesized at the pressure  $p = 7$  GPa and temperature  $T = 800\text{-}1000^\circ\text{C}$ , [9].The tetragonal distortion, which is still large in  $\text{PbV}_{1/2}\text{Fe}_{1/2}\text{O}_3$  (the  $c/a = 1.18$ , placed between the values of 1.23 for  $\text{PbVO}_3$  and 1.06 for  $\text{PbTiO}_3$ ) is considered to be a second order Jahn-Teller effect caused by the electronic configuration of the  $\text{V}^{5+}$  ion and the lone electron pair of the  $\text{Pb}^{2+}$  ion.

In the present work, we will attempt to shed some light on the problem of the effect of partial substitution of V with Fe in of  $\text{PbVO}_3$  compound on magnetic properties by Electron Paramagnetic Resonance (EPR) spectroscopy measurements.

## EXPERIMENTAL

$\text{PbV}_{1-x}\text{Fe}_x\text{O}_3$  ( $0 \leq x \leq 0.75$ ) polycrystalline samples were prepared by solid state reaction under high pressure, high temperature conditions (HP-HT) in a CONAC type apparatus.

For our samples almost single phase samples were obtained at pressures of 6 GPa and temperatures of 950° C, [10,11]. EDX measurements evidenced that the chemical composition of the samples with  $x < 0.5$  were little different from those expected from starting elements.

For samples with  $x < 0.5$  Fe the main phase correspond to the tetragonal structure in the space group  $P4mm$ . The  $a = b$  lattice constants do not depend on the composition and the unit cell height  $c$  decreased linearly with increasing iron content. [10]

X-Ray Absorption Spectroscopy (XAS) data for the vanadium K edge reveals in our samples the presence of  $\text{V}^{4+}$  and  $\text{V}^{5+}$ , and below  $x=0.5$  Fe the composition of the samples can be written as  $\text{Pb}(\text{V}^{4+}_{1-2x}\text{V}^{5+}_x\text{Fe}^{3+}_x)\text{O}_3$  [11]. For  $x = 0.5$  all the  $\text{V}^{4+}$  cations are exhausted and consequently the sample contains only  $\text{V}^{5+}$  and  $\text{Fe}^{3+}$  cations (result consistent with the need / choice of starting oxides). This can also explain why the solid solution stops at  $x = 0.5$ .

Electron Paramagnetic Resonance (EPR) measurements were carried out on a Bruker Elexsys E500 spectrometer in X band (at 9.4 GHz) and in function of temperature.

## RESULTS AND DISCUSSION

EPR was used as an effective tool to study the local magnetic interactions of Vanadium ions. EPR spectra of our  $\text{PbVO}_3$  powder sample show a well-resolved hyperfine structure typical for  $\text{V}^{4+}$  ions, as in fig.11 and reference [11]. The EPR spectra of  $\text{V(IV)}$  ions in an isotropic environment exhibit eight lines of equal peak-to-peak width due to the hyperfine coupling of one unpaired electron ( $S = 1/2$ ) with the nuclear spin ( $I = 7/2$ ) of  $^{51}\text{V}$ . The spectrum shows that both parallel and perpendicular features can be seen.

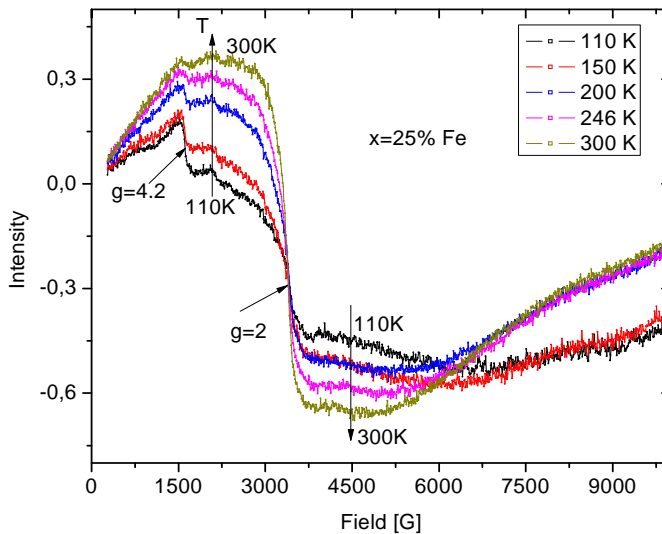
The EPR parameters for  $\text{V}^{4+}$  ions obtained from experimental spectra are consistent with a square–pyramidal  $\text{C}_{4v}$  coordination specific for vanadyl ions [11-16]. The hyperfine coupling constants  $A_{||}$  and  $A_{\perp}$  are sensitive to the local bonding environment for  $\text{V}^{4+}$  coordinated with oxygen ligands.

The small decrease of the hyperfine coupling  $A_{||}$  and  $A_{\perp}$  suggest the slight increase of ligand field with increasing temperature from 110K to 300K [11].

Three signals are invariably reported for  $\text{Fe}^{3+}$  [17-19]: a sharp line around  $g=4.3$ , interpreted as  $\text{Fe}^{3+}$  in a tetrahedral environment with strong rhombic distortion, a broad line around  $g=2.3$  due to oxidic Fe species and a line around  $g=2$ , interpreted as  $\text{Fe}^{3+}$  in (distorted) octahedral environment

The widths of the line are larger in low magnetic fields when compared to high magnetic fields. If the lowest doublet,  $|S_{\pm 1/2}\rangle$  is populated, it gives a  $g$  value of 2 to 6 whereas if the middle Kramer's doublet  $|S_{\pm 3/2}\rangle$  is populated, a  $g$  value 4.30 is expected.

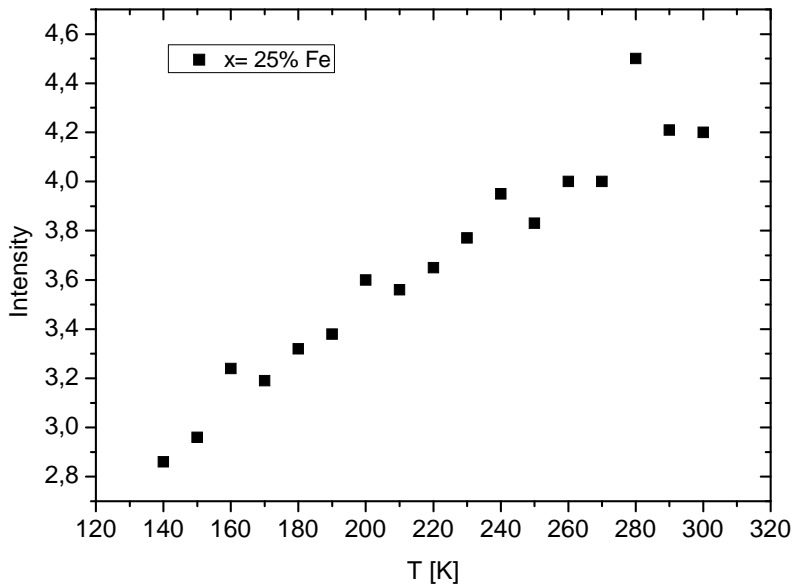
The Fe substitution samples investigated by EPR spectroscopy are  $x=25\% \text{Fe}$  and  $x=40\% \text{Fe}$ . Figure 1 shows the spectra for  $x=0.25$  sample at 5 temperatures (from 300K to 110K). It can be observed that all the resonance spectra exhibit a broad line, centred on  $g = 2$  due to the spin of the  $\text{Fe}^{3+}$  ions. An additional resonant mode is situated around  $g = 4.2$ . By decreasing the temperature the signal around  $g = 4.2$  is well resolved and the signal intensity decreases.



**Fig. 1.** EPR spectra for  $x=25\%$  Fe sample.

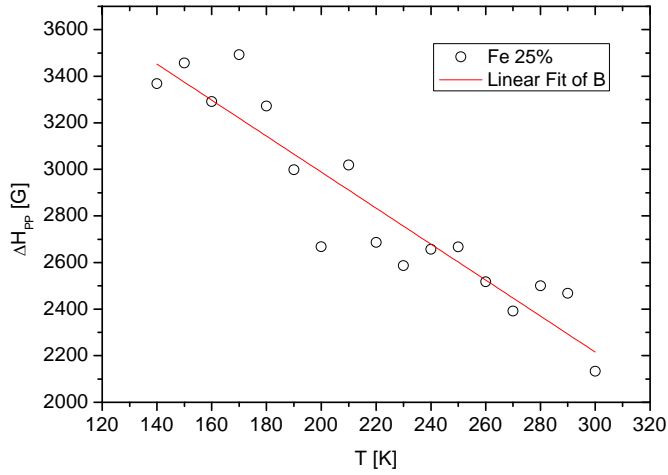
The presence of the additional resonant mode is interpreted as an indication of the presence of  $\text{Fe}^{3+}$  cations in a tetrahedral environment with a strong rhombic distortion.

The complete evolution of the EPR line intensity/concentration of the paramagnetic  $\text{Fe}^{3+}$  centres with the temperature, as determined in the present investigation, is presented in figure 2. One finds that the EPR line intensity of the  $\text{Fe}^{3+}$  paramagnetic centre decreases with decreasing temperature. This suggest the increase of the number of antiferromagnetic  $\text{Fe}^{3+}$ - $\text{Fe}^{3+}$  pairs by decreasing temperature.



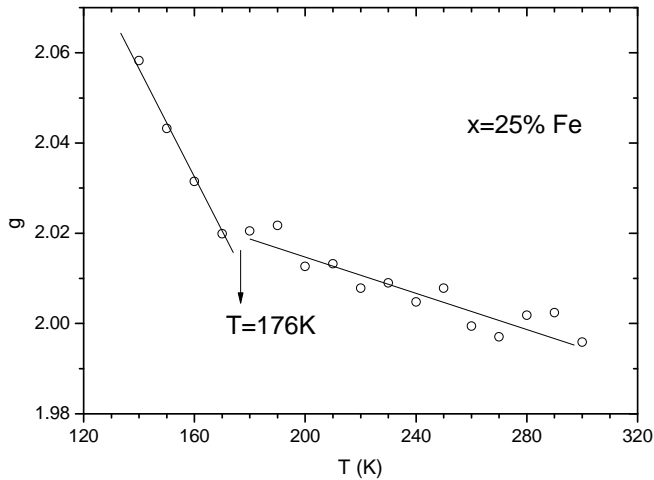
**Fig. 2.** Temperature dependence of the EPR integrated intensity of the  $x=25\%$  Fe sample.

Figure 3 shows that the linewidth  $\Delta H_{pp}$  increases by decreasing temperature. The large value of  $\Delta H_{pp}$  is the result of a strong magnetic dipolar interaction between the  $\text{Fe}^{3+}$  ions [20].



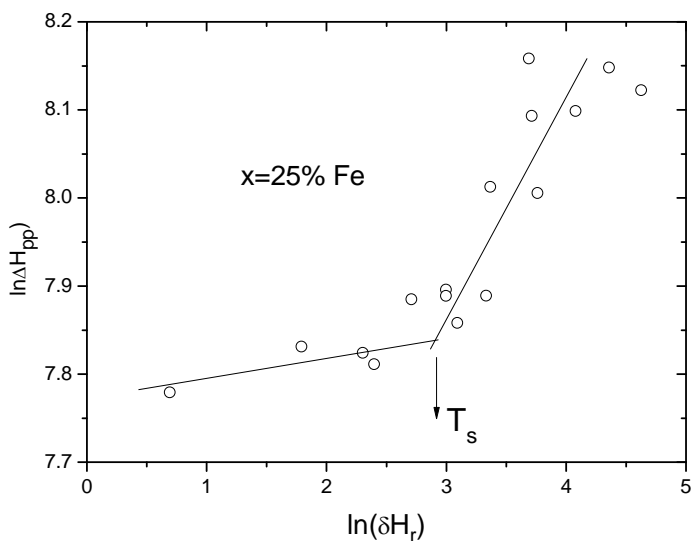
**Fig. 3.** Temperature dependence of the line width in function of temperature for  $x=25\%Fe$  sample.

Figure 4 shows that the  $g$ -factor increases linearly with decreasing temperature, presenting a change of the slope around  $\sim 176$  K. The approximate temperature rate of change for the  $g$ -factor is  $\Delta g/\Delta T \sim 0.17 \cdot 10^{-3} \text{ K}^{-1}$  in the temperature range of 300 to 180 K and  $\Delta g/\Delta T \sim 1.26 \cdot 10^{-3} \text{ K}^{-1}$  (170 –138 K).



**Fig. 4.** Temperature dependence of the  $g$ -factor for  $x=0.25$  sample.

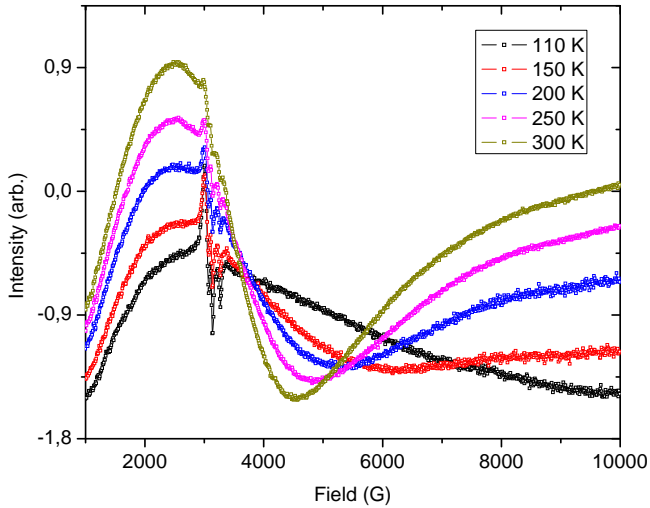
The double logarithmic plot of linewidth  $\Delta H_{pp}$  versus a shift of resonance field  $\Delta H_r$  (see Fig. 5) reveals the existence of two relaxation types with negative slope in the high temperature ranges (300 - 180 K), (175 - 130 K), with a crossover temperature  $T_s$  around 175 K.



**Fig. 5.** Plot of  $\ln(\Delta H_{pp})$  vs.  $\ln(\delta H_r)$  for the  $x=25\%$  Fe sample. The crossover temperature is indicated by the arrow.

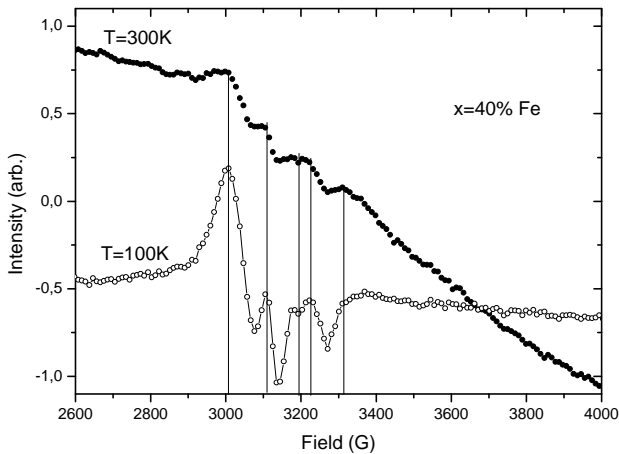
Figure 6 shows the spectra for the  $x=40\%$  Fe sample at the same 5 temperatures as for  $x=25\%$  Fe sample. The signal seems to contain two components: a large transition attributed to  $\text{Fe}^{3+}$  ions (assigned to the central fine structure  $\Delta M_S = -1/2 \rightarrow 1/2$  transition) and a hyperfine structure, respectively.

The EPR line intensity of a paramagnetic centre is proportional with its concentration. For the  $x=40\%$  Fe sample the decrease of the EPR signal with the decreasing temperature shows that the concentration of free  $\text{Fe}^{3+}$  ions decreases. This behaviour is related with the antiferromagnetic order evidenced from magnetic susceptibility measurements.



**Fig. 6.** EPR spectra for the  $x=40\%$  Fe sample at different temperatures.

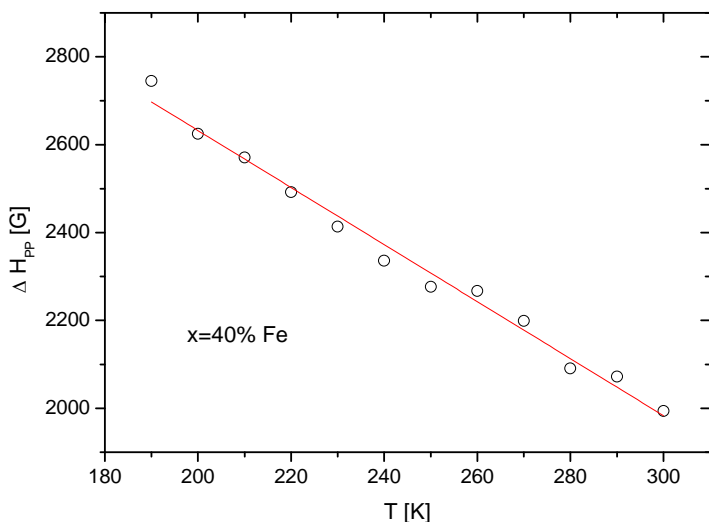
Figure 7 shows that by decreasing the temperature, the hyperfine structure becomes well resolved.



**Fig. 7.** The hyperfine structure of  $x=40\%$  Fe sample at temperatures  $T=300\text{K}$  and  $T=100\text{K}$ , respectively.



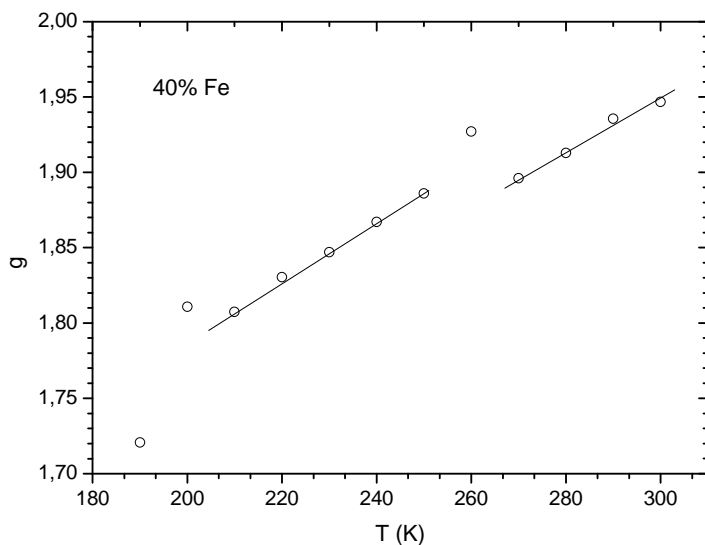
Figure 8 shows that the linewidth  $\Delta H_{pp}$  increases by decreasing temperature with a slope of  $\Delta H_{pp}/\Delta T = -6.5 \text{ G/K}$ , a value lower comparatively with the one obtained for the  $x=25\%$  Fe sample ( $\Delta H_{pp}/\Delta T = -7.7 \text{ G/K}$ ). The large value of  $\Delta H_{pp}$  confirms the presence of a strong magnetic dipolar interaction between the  $\text{Fe}^{3+}$  ions.



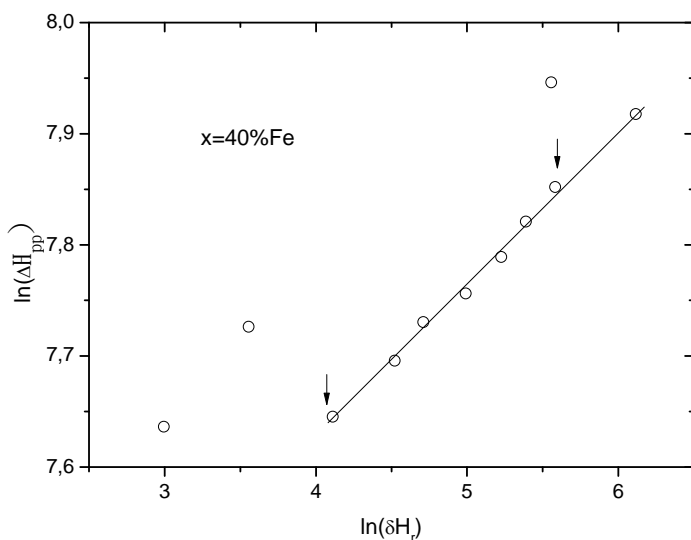
**Fig. 8.** Temperature dependence of the line width function of temperature for  $x=40\%$ Fe sample.

Figure 9 shows that the  $g$ -factor decreases with decreasing temperature, with a noticeable change observed about  $\sim 260 \text{ K}$  and  $200 \text{ K}$ . The temperature change for the  $g$ -factor is  $\Delta g/\Delta T = 1.95 \cdot 10^{-3}$ . The shift of  $g$ -factor and the decrease of  $\Delta H_{pp}$  suggest the increase of the exchange interaction in the sample with  $x=40\%$  Fe comparatively with the  $x=25\%$  Fe sample.

The double logarithmic plot of linewidth  $\Delta H_{pp}$  versus a shift of resonance field  $\Delta H_r$  (see Fig. 10) shows the existence of a single relaxation type with positive slope in the high temperature range (300-200 K).



**Fig. 9.** Temperature dependence of the  $g$  – factor for sample  $x=40\%$  Fe.



**Fig. 10.** Plot of  $\ln(\Delta H_{pp})$  vs.  $\ln(\delta H_r)$  for sample  $x=40\%$  Fe.

Figure 11 shows comparatively the fine structure of the  $\text{PbVO}_3$  ( $x=0.00$  Fe) and of  $x=40\%$  Fe samples. The shift to lower fields of fine structure for  $x=40\%$  Fe sample (PVF\_40) suggest the existence of a different internal field because of the Fe ions. Most likely, the fine structure can be attributed to the vanadium ions.

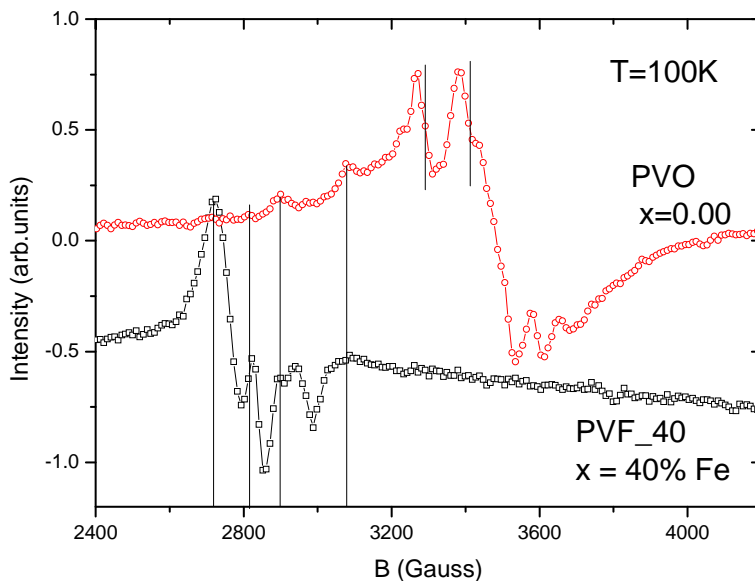


**Fig. 11.** Hyperfine structure of sample  $\text{PbVO}_3$  ( $x=0.0$  Fe) and of the  $x=40\%$ Fe sample.

## CONCLUSIONS

EPR results function of temperature for  $\text{PbVO}_3$  are consistent with the presence of  $\text{V}^{4+}$  paramagnetic ions in a square-pyramidal  $C_{4v}$  coordination (with hyperfine coupling constants  $A_{||}$  and  $A_{\perp}$ ), [11]. The evolution of the hyperfine coupling constants function of temperature is in agreement with the small increase of unit cell height  $c$  with increase of the temperature [10].

All resonance spectra function of temperature, for samples  $x=25\%$  and  $40\%$  exhibit a broad line, centred on  $g=2$  due to the spin of the  $Fe^{3+}$  ions.

For the  $x = 25\%Fe$  sample, an additional resonant new absorption mode situated around  $g=4.2$  was evidenced. It is attributed of the presence of  $Fe^{3+}$  ions on a tetrahedral environment with a strong rhombic distortion.

For sample with  $x=40\%$  Fe, the superimposed hyperfine structure around  $g=2$  can be attributed to the vanadium ions.

The large value of  $\Delta H_{pp}$  is the result of strong magnetic dipolar interaction between the  $Fe^{3+}$  ions in both the  $x=25\%$  and  $40\%$  Fe samples.

The shift of  $g$ -factor and the decrease of  $\Delta H_{pp}$  suggest the increase of the exchange interaction in sample by increasing  $x$ .

The decrease of EPR line intensity attributed to  $Fe^{3+}$  paramagnetic centre with decreasing temperature, suggest the increase of the number of antiferromagnetic pairs  $Fe^{3+}-Fe^{3+}$ .

For the sample  $x=25\%$  Fe two relaxation mechanisms were evidenced with a crossover temperature  $T_s$  around  $175K$ , while for the  $x=40\%$  Fe sample only a single relaxation type is present.

## REFERENCES

1. Shpanchenko R.V., Chernaya V.V., Tsirlin A.A., Chizhov P.S., Sklovsky D.E. and Antipov E.V., 2004, *Chem. Mater.*, 16, 3267-3273.
2. Oka K., Yamada I., Azuma M., Takeshita S., Satoh K.H., Koda A., Kadono R., Takano M. and Shimakawa Y., 2008, *Inorg. Chem.*, 47, 7355.
3. Singh D.J., 2006, *Phys. Rev. B*, 73, 094102.
4. Tsirlin A.A., Belik A.A., Shpanchenko R.V., Antipov E.V., Takayama- Muromachi E. and Rosner H., 2008, *Phys. Rev. B*, 77, 092402.
5. Uratani Y., Shishidou T. and Oguchi T., 2009, *J. Phys. Soc. Jpn.*, 78, 084709.

6. Kumar A., Martin L.W., Denev S., Kortright J.B., Suzuki Y., Ramesh R. and Gopalan V., 2007, *Phys. Rev. B*, 75, 060101.
7. Bonner J.C. and Fisher M.E., 1964, *Phys. Rev.*, 135, A640.
8. Tsuchiya T., Katsumata T., Ohba T. and Inaguma Y., 2009, *J. Ceram. Soc. Jpn.*, 117, 102.
9. Takeshi Tsuchiya, Tetsuhiro Katsumata, Tomonori Ohba, Yoshiyuki Inaguma, *J. of the Ceramic Society of Japan*, 2009, 117, 102-105.
10. Al. Okos, C. Colin, C. Darie, O. Raita, P. Bordet, A. Pop, 2014, *J. Alloys and Compounds*, 602, 265-268.
11. Al. Okos, A. Pop, Céline Darie, P. Bordet, 2013, *Studia UBB Physica*.
12. O.R. Nascimento, C.J. Magon, L.V.S. Lopes, José Pedro Donoso, E. Benavente, J. Páez, Vladimir Lavayen, María Angélica Santa Ana, G. González, 2006, *Molecular Crystals and Liquid Crystals*, Volume 447, Issue 1.
13. O. Cozar, I. Ardelean, I. Bratu, S. Simon, C. Craciun, L. David. C. Cefan, 2001, *Journal of Molecular Structure*, 563-564.
14. A. Agarwall, A. Sheoran, S. Sanghi, V. Bhatnagar, S.K. Gupta, M. Arora, 2010, *Spectrochimica Acta, Part A*, 75.
15. R.P. Sreekanth Chakradhar, A. Murali, J. Lakshmana Rao, 2000, *Physica B*, 293.
16. N. Vedeanu, O. Cozar, I. Ardelean, V. Ioncu, 2007, *J. Opt. Adv. Mat.*, Vol 9, 844-847.
17. Grommen R., Manikandan P., Geometry and Framework Interactions of Zeolite-Encapsulated Copper(II)-Histidine Complexes, 2000, *J. Am. Chem. Soc.*, 122, 11488-11496.
18. Lin D.H., Coudurier G., Vedrine J., Zeolites: Facts, Figures and Future, Proc 8<sup>th</sup> Int. Zeolite Conf., Amsterdam, The Netherlands, July 10–14 1989, Elsevier, Amsterdam, *Stud. Surf. Sci. Catal.*, 49, 1431, 1989.
19. Bert M. Weckhuysen, Ralf Heidler, 2004, Electron Spin Resonance Spectroscopy, *Mol. Sieves*, 4, 295–335.
20. John A. Weil, James R. Bolton, and John E. Wertz, 1994, Electron Spin Resonance: Elementary Theory and Practical Applications - John Wiley & Sons, New York.

